Received: 12 November 2021 | Accepted: 6 June 2022
DOI: 10.1111/2041-210X.13933

Methods in Ecology and Evolution | BRITISH ECOLOGICAL SOCIETY

RESEARCH ARTICLE

Active Remote Sensing for Ecology and Ecosystem Conservation

Vegetation canopy height estimation in dynamic tropical landscapes with TanDEM-X supported by GEDI data

Michael Schlund[1] | Arne Wenzel[2] | Nicolò Camarretta[3] | Christian Stiegler[3] | Stefan Erasmi[4]

[1]Department of Natural Resources, Faculty of Geo-information Science and Earth Observation (ITC), University of Twente, Enschede, The Netherlands

[2]Functional Agrobiodiversity, University of Göttingen, Göttingen, Germany

[3]Bioclimatology, University of Göttingen, Göttingen, Germany

[4]Thünen-Institute of Farm Economics, Braunschweig, Germany

Correspondence
Michael Schlund
Email: m.schlund@utwente.nl

Funding information
Deutsche Forschungsgemeinschaft, Grant/Award Number: 192626868; Ministry of Research, Technology and Higher Education

Handling Editor: Hooman Latifi

Abstract

1. Vegetation canopy height is a relevant proxy for aboveground biomass, carbon stock, and biodiversity. Wall-to-wall information of canopy height with high spatial resolution and accuracy is not yet available on large scales. For the globally consistent TanDEM-X data, simplifications are necessary to estimate canopy height with semi-empirical models based on polarimetric synthetic aperture radar interferometry (PolInSAR).
2. We trained the semi-empirical models with sampled GEDI data, because the assumptions behind the application of such simplifications are not always valid for TanDEM-X. General linear as well as sinc models and empirical parameterizations of these models were applied to estimate the canopy height in tropical landscapes of Sumatra, Indonesia. Airborne laser scanning (ALS) data were consistently used as an independent reference. The general simplified models were compared with the trained empirical versions to assess the potential improvement of the empirical parameterization of the models. The residuals of the different canopy height models were further evaluated in relation to land use and structural information of the vegetation.
3. Our results indicated that the empirical parameters substantially improved the estimation from a root-mean-square-error (RMSE) of 10.3 m (55.8%) to 8.8 m (47.7%), when using the linear model. In contrast, the improvement of the sinc model with empirical parameters was not substantial compared to the general sinc model (7.4 m [40.4%] vs. 6.9 m [37.5%]). A consistent improvement was observed in the linear model, whereas the improvement of the sinc model was dependent on the land-use type. Structural attributes like the canopy height itself and vegetation cover had a significant effect on the accuracies, with higher and denser vegetation generally resulting in higher residuals.
4. We demonstrate the potential of the combined exploitation of the TanDEM-X and GEDI missions for a wall-to-wall canopy height estimation in a tropical region. This study provides relevant findings for a consistent mapping of vegetation

canopy height in tropical landscapes and on large scales with spaceborne laser and SAR data.

KEYWORDS
coherence, GEDI, semi-empirical models, TanDEM-X, tropical landscape, vegetation canopy height

1 | INTRODUCTION

1.1 | Relevance of vegetation canopy height for ecology

Forests are of great importance to the global carbon cycle, where they can be a potential source when disturbed and sink when growing or undisturbed (GCOS, 2015). The quantification of forest biomass as a proxy for carbon and the estimation of its spatial distribution supports our understanding of the role of forests in climate change and its mitigation. The vegetation canopy height is a relevant proxy for aboveground biomass and other structural attributes of vegetation (Asner & Mascaro, 2014; Dubayah et al., 2020; Réjou-Méchain et al., 2015). Furthermore, canopy height and its heterogeneity are considered as indicators for ecosystem structure and its complexity as an essential biodiversity variable (Atkins et al., 2021; Fahey et al., 2019; Lang et al., 2022). For instance, it was found that information about the spatial distribution of canopy height supports the prediction of biodiversity variables on global scale (Feng et al., 2020; Gatti et al., 2017).

Mapping canopy height as an essential biodiversity variable (EBV) over large areas requires the use of remote sensing (Skidmore et al., 2021). This is particularly true in vast areas with limited access, such as tropical forests. In general, active remote sensing (i.e. light detection and ranging [LiDAR] and synthetic aperture radar [SAR]) is considered to have high potential for the estimation of canopy height and aboveground biomass (Asner & Mascaro, 2014; Dubayah et al., 2020; Quegan et al., 2019; Réjou-Méchain et al., 2015). Airborne laser scanning (ALS) data have normally only limited spatial coverage and are expensive compared to spaceborne data. In order to provide consistent information about canopy height beyond the local scale, spaceborne LiDAR and SAR data are necessary. The existing wall-to-wall estimations of vegetation canopy height on regional to global scale were generally associated with high uncertainties and coarse spatial resolution (Dubayah et al., 2020; Lang et al., 2022; Quegan et al., 2019). The potential of spaceborne LiDAR and SAR sensors resulted in the development and launch of different spaceborne missions dedicated to estimate ecosystem structure (Dubayah et al., 2020; Fatoyinbo et al., 2021; Quegan et al., 2019). The Global Ecosystem Dynamics Investigation (GEDI) mission is a spaceborne LiDAR, which was launched in late 2018 and is specifically designed to estimate vegetation structure with a sampling grid resulting in a total coverage of the global land surface of 4% (Dubayah et al., 2020; Lang et al., 2022). The exploitation and fusion of GEDI with current and future missions can result in an accurate wall-to-wall estimation of canopy height and aboveground biomass on potentially global scale (Dubayah et al., 2020; Fatoyinbo et al., 2021; Qi et al., 2019; Quegan et al., 2019; Silva et al., 2021).

1.2 | Estimation of canopy height with SAR data

Empirical or semi-empirical models using interferometric SAR (InSAR) or polarimetric InSAR (PolInSAR) techniques have been frequently exploited to estimate canopy height (Karila et al., 2015; Khati et al., 2018; Kugler et al., 2014; Lindgren et al., 2017). Two-layer models like the Random Volume over Ground (RVoG) model are typically used to estimate canopy height and consist of a volume and an impenetrable ground layer. This model is considered to have a high potential in the estimation of canopy height from SAR data, because it links the SAR measurements with the canopy height (Cloude & Papathanassiou, 2003; Kugler et al., 2014; Quegan et al., 2019). Short wavelengths, like the C- and X-band, are successfully exploited for the canopy height estimation. The InSAR heights were frequently combined with data of the ground elevation to estimate the height of the canopy assuming that the penetration into the volume layer (i.e. vegetation) is negligible (Schlund et al., 2020; Solberg et al., 2013). The assumption of negligible penetration in X-band is generally not valid and thus different modelling approaches are needed to estimate vegetation canopy height (Kugler et al., 2014; Qi et al., 2019; Qi & Dubayah, 2016; Schlund et al., 2020).

The TanDEM-X mission provides data with minimal temporal decorrelation, which makes this mission particularly useful for global InSAR applications (Krieger et al., 2007). Empirical and semi-empirical models, like the RVoG model, were exploited in the canopy height estimation using TanDEM-X (Karila et al., 2015; Khati et al., 2017; Kugler et al., 2014; Lindgren et al., 2017; Olesk et al., 2016). Most TanDEM-X data are acquired in single-polarization and thus the RVoG model requires simplifications to estimate canopy height (Chen et al., 2016; Chen et al., 2021; Olesk et al., 2016; Schlund et al., 2019). The necessity to simplify this model is based on the fact that it requires a sufficient number of observations from the ground layer scattering and from the vertical structure of the volume layer, which are normally provided by the different polarizations (Cloude & Papathanassiou, 2003; Quegan et al., 2019). The simplification results in a sinc model and the canopy height estimation with simplified RVoG models (i.e., linear and sinc model) resulted in accuracies of 5–14 m in boreal and temperate forests

(Schlund et al., 2019). It can be assumed that the simplifications are not always valid and empirical adjustments were proposed (Gómez et al., 2021; Olesk et al., 2016). It was suggested that ALS data have the potential to train the empirical parameters (Gómez et al., 2021). To date, most studies have used either the general simplified models with or without parametrization, but the two appraoches were not compared to assess the relevance of the empirical adjustments (Gómez et al., 2021; Olesk et al., 2016; Schlund et al., 2019). Based on the limited coverage and availability of ALS data, particularly in the tropics, their application for training the TanDEM-X canopy height estimation models is limited. In addition, ALS data acquisitions have to be temporally consistent with the TanDEM-X acquisition to train the empirical parameters. Spaceborne LiDAR data, like the Global Ecosystem Dynamics Investigation (GEDI) mission, provide canopy height information on a global scale with high temporal resolution (Dubayah et al., 2020). The potential of combining GEDI and TanDEM-X data has been shown (Qi et al., 2019; Qi & Dubayah, 2016), where the GEDI data was simulated from ALS data. GEDI is a sampling mission with point-wise measurements and thus does not provide wall-to-wall ground elevation and canopy height with high resolution (Dubayah et al., 2020). Nevertheless, sampled GEDI data can be used to train the empirical parameters of the simplified canopy height estimation models of TanDEM-X at the GEDI footprints for a wall-to-wall coverage on regional scales. Potapov et al. (2021) trained bagged regression trees with GEDI and Landsat data to estimate canopy height on large scale. However, it can be assumed that InSAR data is more sensitive to the vertical structure of vegetation than optical data (Karila et al., 2015; Khati et al., 2018; Kugler et al., 2014; Olesk et al., 2016). The simplified semi-empirical models based on InSAR data were considered to have high potential to estimate canopy height, although their potential improvement by using them with GEDI data was to date not assessed, in particular in tropical forests.

The objective of this study was to assess the potential of the simplified canopy height estimation models based on TanDEM-X and to evaluate the performance difference between the simple general models and their empirical parameterizations. The linear and sinc model were assessed as simplifications of the RVoG model. The models were compared to canopy height retrievals of a model with additional ground elevation information from GEDI. A similar approach achieved highest accuracies in Qi et al. (2019), which used simulated GEDI data. Existing studies have only applied the simple models in higher latitude forests (Chen et al., 2016, 2021; Gómez et al., 2021; Olesk et al., 2016), whereas we study the models in a dynamic tropical landscape with different types of land use such as forest, mono-cultural rubber and oil palm plantations. In contrast to other studies, in which ALS data were used for training and reference (Chen et al., 2021; Gómez et al., 2021; Guliaev et al., 2021; Qi et al., 2019), the training of the empirical parameters in our study is conducted with GEDI data. GEDI data are substantially different compared to ALS data in terms of acquisition concept, spatial coverage, accuracy and spatial detail (Adam et al., 2020; Dubayah et al., 2020). The potential of actual GEDI data to support TanDEM-X-based canopy height estimations has not been assessed yet. The simplified models used in this study are independent of the ground elevation, which is contrary to other studies (Guliaev et al., 2021; Lei et al., 2021; Qi et al., 2019). This independence from ground elevation and training with spaceborne GEDI data overcomes the current limits of TanDEM-X based canopy height estimations and facilitates the application of the canopy height estimation on regional to even global scales. The results of our study provide information about the performance difference and potential improvement of different simplification levels of the canopy height estimation models. Consequently, this study contributes relevant findings in the combined exploitation of the TanDEM-X and GEDI mission for vegetation canopy height assessment on a regional scale with wall-to-wall coverage.

2 | MATERIALS AND METHODS

2.1 | Study area

The study area covers a tropical lowland area in the Jambi province, Sumatra, Indonesia (Figure 1). It has a tropical humid climate, with relatively constant temperatures and a drier period during July and August. The study area was part of a long-term interdisciplinary research project that investigates the ecological and socioeconomic effects of land-use transformation in a tropical lowland area. It covered a mosaic of land-use systems such as forests, shrubland as well as plantations of oil palm *Elaeis guineensis* and rubber *Hevea brasiliensis* (Clough et al., 2016), which are assumed to be relatively equally distributed in the area. These land-use systems are representative for the complex tropical landscapes of Indonesia and are significantly different in their ecological functions (Drescher et al., 2016).

2.2 | TanDEM-X data

The TanDEM-X mission consists of two X-band SAR sensors, with a wavelength of 3.1 cm. The main objective of this mission is to create multiple global digital elevation models (DEM) with single-pass InSAR data (Krieger et al., 2007; Lachaise et al., 2019).

The data used in this study were acquired in horizontal polarization (transmit and receive; HH) and StripMap mode. This mode resulted in a spatial resolution of about 3 m. The heights of ambiguity were between 46.6 and 76.3 m (Table 1). The co-registered single-look slant range complex (CoSSC) data products were used for this study, in which the data were spectrally filtered in azimuth and range as well as co-registered and resampled (Fritz, 2012).

2.3 | LiDAR data

A full-waveform and a multi-discrete return LiDAR were utilized in this study. First, the full-waveform GEDI data were used to train the

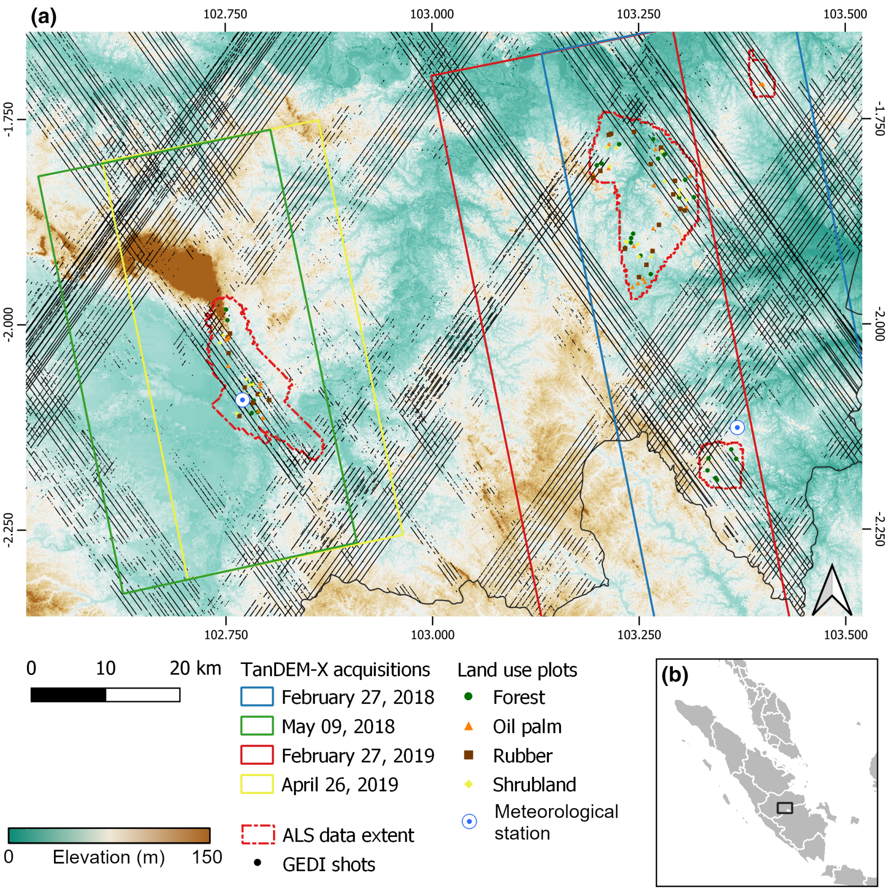

FIGURE 1 Overview of the study area with the extent of the TanDEM-X acquisitions and the ALS data, GEDI shots and location of land use plots with the global TanDEM-X digital elevation model in the background (a) on the island of Sumatra, Indonesia (b).

TABLE 1 Overview of TanDEM-X datasets and sum of precipitation 3 days before and at the acquisition date retrieved from stations within the respective coverage (incidence angle θ and height of ambiguity (HoA) stand for the parameter at scene centre)

Acquisition date	θ (°)	Resolution (m) azimuth × range	HoA (m)	Precipitation (mm)
27 February 2018	33.8	3.3×3.2	76.3	37.7
9 May 2018	46.2	3.3×2.4	73.9	0.9
25 February 2019	32.4	3.3×3.3	46.6	5.3
26 April 2019	34.9	3.3×2.4	46.8	72.8

models to estimate vegetation canopy height based on TanDEM-X. This LiDAR sampling mission was installed on the International Space Station (ISS) in 2018 to provide information of the vertical structure of vegetation on a global scale (Dubayah et al., 2020). Level 2A Elevation and Height Metrics (v002) data were exploited, in which the ground elevation and relative height (RH) metrics were derived from the LiDAR waveform on a footprint resolution of 25 m (Dubayah et al., 2020, 2021). GEDI data acquired between 15 May 2019 and 6 June 2020 were used, since these GEDI acquisitions were in general temporally and spatially consistent with the TanDEM-X and ALS acquisitions of this study (Figure 1).

Second, ALS data were available for four different areas in the Jambi province (Figure 1). The ALS data covered representative land-use systems of the province, with oil palm and rubber plantations of small-holders and large estates, shrublands and fragmented forests as well as protected areas of forests. A Riegl Q780 full waveform scanner was used to acquire the data in January and February 2020. The scanning resulted in a nominal pulse density of 15 points/m^2 with a vertical accuracy of ≤10 cm according to the data provider. The ALS data covered approximately 6% (i.e. 420 km^2) of the TanDEM-X acquisitions (7,430 km^2; Figure 1) and were used as reference data for model validation in this study.

2.4 | Auxiliary data

Accurate information about the land use was available for 99 circular plots with a size of 1,000 m^2. Four land-use types with an almost equal distribution were covered in these plots: forest ($n = 27$), rubber ($n = 25$), oil palm ($n = 25$), and shrubland ($n = 22$). These four land-use systems were the most dominant land uses in central Sumatra (Grass et al., 2020). These land-use types were found to be highly significant in the variation of ecological functions (e.g. carbon stock and flux) and biodiversity (Clough et al., 2016; Grass et al., 2020; Guillaume et al., 2018). Surveying these four systems provides an exhaustive sample of the major ecological and socioeconomic impacts of rainforest transformation in central Sumatra, and by extension in many similar regions in South-East Asia (Drescher et al., 2016; Grass et al., 2020).

Forests were dominated by trees with a canopy cover at minimum of 50%, whereas shrublands were fallow lands with a canopy cover up to 50%. Shrublands constitute lands after deforestation that lay fallow for a few years before being developed to a plantation (Grass et al., 2020). Despite their transitional character, they are an important landscape component that have value for biodiversity or ecosystem functioning. Oil palm and rubber were plantations of the respective tree or crop. For further details on the individual land-use systems and their ecological and socio-economic significance in the study area, for example Drescher et al. (2016); Guillaume et al. (2018); Clough et al. (2016); Grass et al. (2020).

Meteorological data were acquired from different stations in the study area (Figure 1). It can be assumed that dry conditions are favourable for the canopy height estimation with TanDEM-X (Schlund et al., 2019). Therefore, the sum of the precipitation 3 days prior to and on the day of acquisition was retrieved from the stations, which were located within the respective TanDEM-X acquisition. At each station, precipitation was measured with two precipitation transmitters (Thies Clima) at 1.5 m height and horizontal separation of about 6 m. Measurements were acquired every 15 s as well as averaged and stored on a DL16 Pro data logger (Thies Clima) every 10 min (Meijide et al., 2018).

The acquisition of the data was funded by the Deutsche Forschungsgemeinschaft (DFG, German Research Foundation)—project number 192626868—SFB 990 and the Ministry of Research, Technology and Higher Education (Ristekdikti) in the framework of the collaborative German–Indonesian research project CRC990, subprojects A03, B09 and Z02. Additional licences and permits were not required.

2.5 | Methods

2.5.1 | Canopy height estimation with ALS and GEDI

The GEDI Level 2A data were extracted for the Jambi province. Only data that fulfilled the quality criteria of the GEDI mission (i.e. quality flag of 1) and had a sensitivity of 0.9 or higher were used (Adam et al., 2020; Dubayah et al., 2021). In total, about 90,000 subsetted GEDI shots were located in the TanDEM-X coverages and about 6,000 shots were located over the scanned area with ALS flights. The lowest elevation, as well as the relative height (RH) values were extracted from the subsetted GEDI data.

Canopy heights were calculated from ALS point cloud data, where the point clouds were first classified into ground and non-ground points. Outliers within the point clouds were removed and a ground layer was retrieved by triangulating the ground points. The canopy height was calculated by sampling the highest z-value of the point cloud within a 25 m cell above the ground layer. This information was further triangulated from the point cloud to result in a raster product with 25 m pixel spacing. The 25 m pixel size was used for consistency with the footprint and spatial resolution of GEDI. The highest point of ALS point clouds was frequently used as a reference in other studies in which canopy heights were analysed from InSAR data (Caicoya et al., 2016; Kugler et al., 2014; Schlund et al., 2019). It was assumed that the highest z-value above the ground corresponds best with the RH100 height from GEDI representing vegetation canopy heights (Adam et al., 2020). Different relative height (RH) metrics were compared against the ALS based canopy height to confirm this assumption. Moreover, the ground elevation as the elevation of the lowest mode from the GEDI waveform was compared to the ALS ground elevation.

Various ALS metrics were also extracted from the point cloud for the plots and for the whole landscape. The metrics were the standard deviation of the heights of points, the effective number of layers (Ehbrecht et al., 2016), the canopy surface roughness expressed by the rumple index (Parker et al., 2004) and vegetation cover, calculated as the ratio of points above 2.5 m compared to all points within a 1,000 m^2 plot. These metrics were used because they were considered important for characterizing the vertical and horizontal vegetation structure and the heterogeneity of these land uses (Camarretta, Ehbrecht, et al., 2021).

2.5.2 | Canopy height estimation with TanDEM-X

The interferometric coherence was retrieved with a multi-looking to obtain a 25 m spatial resolution in each TanDEM-X acquisition, corresponding to the footprint and spatial resolution of the GEDI heights. The volume coherence γ_{Vol} was extracted by taking into account the signal-to-noise ratio γ_{SNR} in the total coherence γ (Kugler et al., 2014; Schlund et al., 2019). It can be assumed that there is a relationship between the volume coherence γ_{Vol} and the vegetation canopy height, which can be exploited with the RVoG model (Cloude & Papathanassiou, 1998, 2003; Papathanassiou & Cloude, 2001; Quegan et al., 2019). Consequently, this model is also utilized in our study.

Based on the number of parameters in this model, full-polarimetric data are required to invert it. The global TanDEM-X data are generally acquired in HH polarization and thus simplifications are necessary to estimate canopy height (Kugler et al., 2014; Olesk et al., 2016; Schlund et al., 2019). The simplifications were frequently based on the assumption that the ground contribution in the TanDEM-X data is negligible. Furthermore, the extinction of the signal was assumed to be zero in previous studies that used TanDEM-X data to estimate canopy height (Kugler et al., 2014; Olesk et al., 2016). This results in a sinc model for the $|\gamma_{\mathrm{Vol}}|$,

$$\left|\gamma_{\mathrm{Vol_{sinc}}}\right| = \left|\mathrm{sinc}\left(\pi \frac{h_V}{\mathrm{HoA}}\right)\right| = \left|\frac{\sin\left(\pi \frac{h_V}{\mathrm{HoA}}\right)}{\pi \frac{h_V}{\mathrm{HoA}}}\right|, \tag{1}$$

where the vegetation height h_V is related to the InSAR height sensitivity expressed by the height of ambiguity (HoA $= 2\pi/k_z$). It can be assumed that no canopy height results in a volume coherence $|\gamma_{Vol}|$ of 1. A canopy height that is equal to the height of ambiguity results in a volume coherence $|\gamma_{Vol}|$ of 0. Consequently, a linear relationship between canopy height and TanDEM-X coherence can be utilized (Olesk et al., 2016; Schlund & Boehm, 2021; Treuhaft et al., 2015),

$$\left|\gamma_{\mathrm{Vol}_{\mathrm{linear}}}\right| = \left|1 - \frac{h_V}{\mathrm{HoA}}\right|. \quad (2)$$

As mentioned above, it was found that these assumptions of the simplifications are often not valid and thus empirical parameters in the simplified models are suggested to accurately estimate canopy height (Gómez et al., 2021; Olesk et al., 2016; Schlund & Boehm, 2021),

$$\left|\gamma_{\mathrm{Vol}_{\mathrm{sinc}_{\mathrm{Empirical}}}}\right| = a\left|\mathrm{sinc}\left(b_{\mathrm{sinc}}\pi\frac{h_V}{\mathrm{HoA}}\right)\right| \quad (3)$$

and

$$\left|\gamma_{\mathrm{Vol}_{\mathrm{linear}_{\mathrm{Empirical}}}}\right| = \left|a - b_{\mathrm{linear}}\frac{h_V}{\mathrm{HoA}}\right|, \quad (4)$$

where a and b are the empirical parameters for the sinc and linear models, respectively.

The sinc and linear models without empirical parameters suggest that no canopy height results in a $|\gamma_{Vol}|$ of 1. Any non-volume decorrelation decreases the estimated $|\gamma_{Vol}|$ and the empirical parameter a takes into account that the retrieved $|\gamma_{Vol}|$ was potentially not purely related to the volume. The cumulative density of $|\gamma_{Vol}|$ values at valid GEDI shots was calculated. The parameter a was retrieved where the cumulative density function saturated (Chen et al., 2016). Note that a was independent from the model, resulting in a similar value for linear and sinc models.

A potential ground contribution and a non-zero extinction of the signal result in different vertical profiles (Gómez et al., 2021). It is not possible to determine the ground-to-volume ratio and extinction as parameters of the RVoG model with the single-polarized TanDEM-X data. The GEDI RH100 heights were used to fit the linear and sinc models with the estimated $|\gamma_{Vol}|$ to retrieve the parameter b. The parameterization of a and b was conducted for each individual TanDEM-X acquisition. Finally, the linear and sinc models with and without empirical parameterization were inverted to estimate the vegetation canopy height.

Numerous studies have suggested that information about the ground height requires fewer simplifications in the models for canopy height estimation (Chen et al., 2016; Khati et al., 2018; Kugler et al., 2014; Qi et al., 2019; Qi & Dubayah, 2016). It is not possible to estimate the ground elevation with TanDEM-X and thus external information (e.g. ALS data) must be used to estimate the phase of the ground elevation ϕ_0 (Chen et al., 2016; Khati et al., 2018; Kugler et al., 2014). The phase of the ground elevation ϕ_0 was extracted from GEDI as lowest elevation in our study. This was combined

TABLE 2 Summary of the different models and their TanDEM-X and GEDI inputs used in this study with their relative RMSE, bias and R^2 (Simplified RVoG with ground information is used as benchmark in GEDI footprints; all were significantly different)

Model	Parametrization	TanDEM-X metric	GEDI metric	Parameters	RMSE	Bias	R^2
Linear	None	Coherence magnitude	—	$\frac{h_V}{\mathrm{HoA}} = 0$ equals $\|\gamma_{Vol}\|$ of 1; $\frac{h_V}{\mathrm{HoA}} = 1$ equals $\|\gamma_{Vol}\|$ of 0	55.76	−39.73	0.43
Linear	Empirical	Coherence magnitude	CHM	Parameters were found empirically with GEDI	47.65	1.53	0.46
Sinc	None	Coherence magnitude	—	No ground contribution; zero extinction	40.38	11.45	0.47
Sinc	Empirical	Coherence magnitude	CHM	Parameters were found empirically with GEDI	37.49	−6.32	0.50
Simplified RVoG with ground information	Empirical	Complex coherence	CHM & DTM	Ground pase from GEDI DTM; other parameters were found empirically from GEDI CHM	35.83	1.99	0.53

with the volume coherence γ_{Vol} of TanDEM-X to estimate canopy height (Chen et al., 2016; Khati et al., 2018; Qi et al., 2019; Schlund et al., 2019). This means that the best case scenario from Qi et al. (2019) using the canopy height and ground elevation as input was adapted to the GEDI footprints in our study. This was compared with the simple models to indicate the performance differences of the various levels of simplification. The different models are summarized in Table 2.

2.5.3 | Validation of the canopy height estimations

The ALS canopy height was used as an independent validation dataset. This was based on the assumption that the vertical accuracy of ALS was very high compared to the accuracy of TanDEM-X. In order to assess the accuracy, the coefficient of determination R^2, root-mean-squared error (RMSE) and bias were calculated for the individual TanDEM-X scenes and for all scenes combined. The relative RMSE and bias were further calculated with the average of the canopy height from ALS. In addition, the residuals of the different canopy height estimations were calculated as the difference between TanDEM-X and ALS-based canopy height (considered as reference) for all available pixels as well as in the land-use plots. The residuals were further normalized with respect to the ALS canopy height. The significance of differences between the residuals of the used models was assessed using Tukey's honest significance test (Miller, 1981). In addition to the land-use types, the residuals were stratified for the whole landscape by canopy height in a 5 m interval and canopy cover in a 10% interval.

The assumptions of no ground contribution and zero extinction were further analysed in the land-use plots. The proportion of land-use plots where the estimated volume coherence $|\gamma_{Vol}|$ was lower than the modelled volume coherence $|\gamma_{Vol_{sinc}}|$ was extracted ($P[|\gamma_{Vol}|<|\gamma_{Vol_{sinc}}|]$). It can be assumed that significant extinction was present if the estimated volume coherence $|\gamma_{Vol}|$ was higher than the modelled coherence $|\gamma_{Vol_{sinc}}|$ from Equation (1) (Chen et al., 2021; Praks et al., 2012; Schlund et al., 2019).

The volume is normally assumed as infinitely deep without ground contribution of the SAR signal if the height of the scattering phase centre is above half of the actual canopy height (Dall, 2007; Praks et al., 2012). The scattering phase centre height was extracted as the difference between the interferometric SAR height h_{InSAR} above the ground phase. The ALS ground height was used to extract the ground phase for this purpose. Again, the proportion of land use plots in which the InSAR height was higher than half of the ALS canopy height model was calculated ($P[h_{InSAR} > CHM/2]$), where the ALS canopy height was considered as the actual canopy height. This indicated the proportion of land-use plots with negligible ground contribution.

The ALS metrics—namely canopy height, vegetation cover, ENL, rumple and standard deviation of heights—were used in a multiple-linear regression in order to assess the impact of different structural parameters on the residuals. The ALS metrics used in this regression were scaled prior to the fit of the model to a mean of 0 and a standard deviation of 1. Consequently, the coefficients provided information about the relative strength of the variables in this model.

3 | RESULTS

3.1 | Comparison of GEDI and ALS canopy heights

The ground elevation was estimated from GEDI with an RMSE of 4.9 m, where a subtle positive bias of 0.7 m was observed compared to the ALS ground elevation (Figure 2a). Both LiDAR-based canopy heights revealed overall an average vegetation canopy height of about 19 m. The average canopy height based on GEDI data was 18.9 m with a standard deviation of 10.6 m. The average ALS-based canopy height was 19.5 m with a standard deviation of 9.7 m. The comparison of the GEDI RH100 and ALS canopy height revealed a relationship with an R^2 of 0.4. The RMSE was 8.8 m, which equaled 44.9% with respect to the mean ALS canopy height (Figure 2b). The bias of the RH100 was minimal with −0.8 m (−4%) compared to other relative heights.

3.2 | Coherence modelling & canopy height estimation

The comparison of estimated volume coherence $|\gamma_{Vol}|$ and GEDI RH100 height, normalized with the respective height of ambiguity

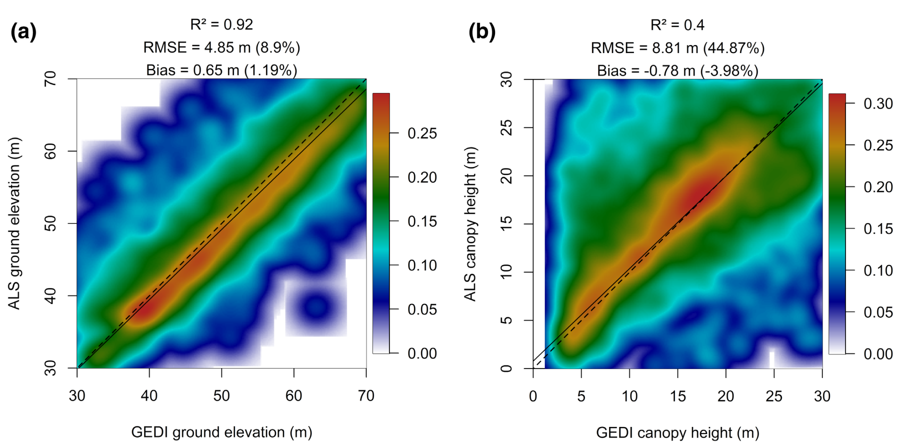

FIGURE 2 Scatterplot with coloured density of GEDI and ALS ground elevation (a) and GEDI RH100 and ALS canopy height (b; with 1:1 [dashed] and regression line [solid]).

(HoA), revealed that zero canopy heights generally resulted in a coherence lower than 1. This was confirmed by the *a* values for the different acquisitions. In general, the estimated coherence decreased with increasing canopy height. This is also indicated in the models, where largest discrepancies between the model and the observations were observed for the linear model without empirical parameterization. The discrepancies were substantially reduced with the empirical parameterization, in particular for the linear model (Figure 3). The effect of the height of ambiguity was visible in Figure 3, in which the acquisitions with larger heights of ambiguity generally resulted in lower normalized canopy heights (Figure 3a,b).

When the TanDEM-X-based canopy heights of the individual acquisitions were pooled together, the empirical sinc model achieved the best results compared to the other models. The R^2 in the comparison of estimated heights from TanDEM-X and ALS was 0.5 and the RMSE was 6.9 m (37.5%) with a bias of −1.2 m (−6.3%) (Table 2). Compared to the general sinc model, the model with empirical parameterization resulted in an improvement of 0.03 and 0.5 m (2.9%) for the R^2 and RMSE, respectively. The absolute bias decreased from 11.5% to 6.3%. For the linear model, the empirical parameterization improved the RMSE by 1.5 m (i.e. 8.1%) in the linear model and the absolute bias decreased from 39.7% to 1.5% (Table 2). In general, the sinc models resulted in higher accuracies in terms of R^2 as well as RMSE and the regression line followed the 1:1 line closer compared to the linear models (Figure 4).

The estimation of canopy height with the simple models achieved lower accuracies compared to the model with additional ground phase information, which was retrieved from the GEDI ground elevation (Table 2). The R^2 of the model with ground elevation information was 0.53. The RMSE of the model with ground elevation information was 6.1 m (35.8%) and thus lower as compared to the best simple model. The bias was 0.3 m (2.0%) for the model with ground elevation information (Table 2).

Similar results compared to the pooled data were observed for the individual acquisitions (Table 3). The sinc model with empirical parameterization achieved the highest accuracies in terms of RMSE, bias and R^2. However, the smallest improvement of RMSE and R^2 was observed for the acquisition from 25 February 2019, while the bias improved substantially. The biggest improvement of RMSE, bias and R^2 was observed for the acquisition from 9 May 2018. In general, the empirical parameterization improved the results substantially in the linear model (Table 3).

The spatial distribution of the estimated canopy height revealed large canopy heights up to 40 m and more, particularly in the north-west but also in the south-east of the study area (Figure 5). Most of the other areas had a canopy height between 10 and 30 m. Some regular patterns of low canopy heights were observed in the centre of the eastern TanDEM-X acquisitions with canopy heights below 10 m, which represented large oil palm plantations (Figure 5). The areas in Figure 5a and c were mainly covered by smallholder plantations of rubber and oil palm. Only some fragments of forest and shrubland were located in these areas. In contrast, forests were located in the north of Figure 5a and in particular in Figure 5b. A moderate underestimation of the canopy heights was indicated in these forested areas by the difference of the TanDEM-X and the ALS-based canopy heights. The other areas of small-holder plantations and fragmented forests indicated no

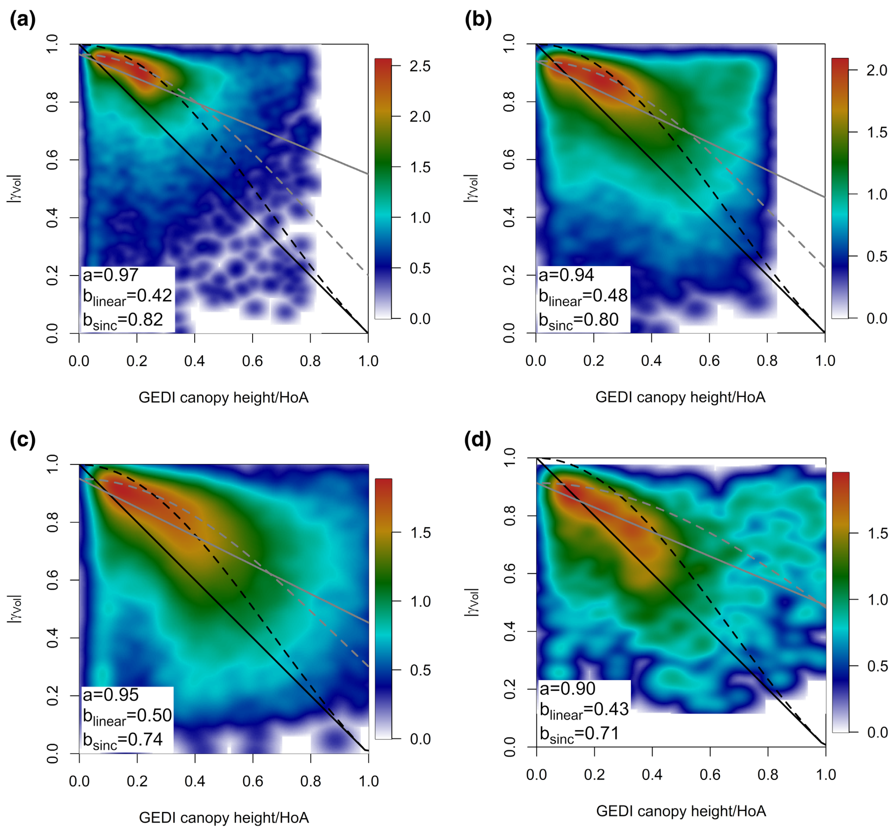

FIGURE 3 Scatterplots with coloured density of TanDEM-X coherence from 27 February 2018 (a), 9 May 2018 (b), 25 February 2019 (c) and 26 April 2019 (d) and GEDI RH100 canopy height (normalized with the height of ambiguity) with lines of different coherence models (black solid line = linear model without empirical parameterization; grey solid line = linear model with empirical parameterization; black dashed line = sinc model without empirical parameterization; grey dashed line = sinc model with empirical parameterization).

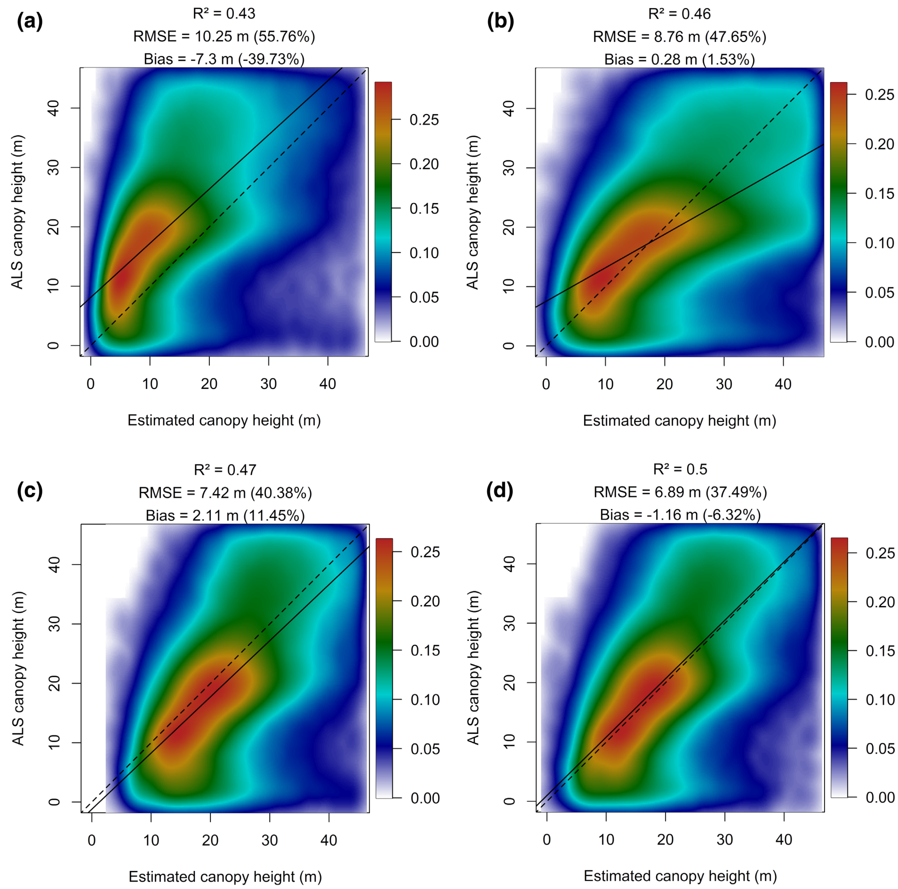

FIGURE 4 Comparison of ALS canopy height and estimated canopy height with linear model without empirical parameterization (a) and with empirical parameterization (b) as well as with sinc model without empirical parameterization (c) and with empirical parameterization (d) for all acquisitions combined (with 1:1 [dashed] and regression line [solid]) (All were significantly different).

TABLE 3 Accuracy of canopy height estimation for the individual acquisitions with R^2, relative RMSE and bias in % (emp. Stands for empirical parameterization, Acqu. for acquisition and Feb. for February)

	Linear			Linear emp.			Sinc			Sinc emp.		
Acqu. date	R^2	RMSE	Bias	R^2	RMSE	Bias	R^2	RMSE	Bias	R^2	RMSE	Bias
27 Feb. 2018	0.49	58.6	−49.5	0.49	44.1	−6.1	0.51	36.1	8.2	0.52	34.3	−0.8
9 May 2018	0.42	54.8	−37.5	0.46	45.3	0.7	0.45	50.1	27.6	0.50	39.9	5.6
25 Feb. 2019	0.44	55.3	−44.1	0.49	47.8	−4.3	0.59	33.8	−17.4	0.62	32.2	−4.2
26 April 2019	0.45	57.6	25.4	0.45	50.1	−19.2	0.46	49.9	20.7	0.50	47.7	−13.0

particular under- or overestimation (Figure 5). The only exception was a substantial overestimation in the east of Figure 5a. This was due to the temporal difference between TanDEM-X and ALS acquisitions, in which an oil palm plantation was harvested between the acquisitions.

3.3 | Accuracy of canopy height estimation with respect to vegetation structure

The linear regression of the canopy height estimation residuals and different ALS metrics revealed that the canopy height as well as vegetation cover had a significant impact on the residuals. The canopy height was not significant for residuals of the sinc model without empirical parameters, whereas the vegetation cover was not significant for either of the linear models. The coefficient of the canopy height was substantially higher than the other coefficients, except for the sinc model (Table 4). This confirmed the overall dependency of the residuals on the canopy height.

The coefficients for the vegetation cover tended to be negative, which indicated that lower vegetation cover in combination with canopy height resulted in higher residuals (Table 4). This was confirmed visually when the mean of the four land use types was considered in the visual representation of these relationships (Figure 6). The R^2 of the relationship between the residuals and forest structure parameters from ALS was the highest for the sinc model with empirical parameters (R^2 = 0.38) and the linear model without empirical parameters (R^2 = 0.40). This suggested that about 40% of the variation of the residuals could be explained with these ALS metrics (Table 4). All available plots were considered for these relationships (Table 4), whereas in the scatterplots the mean and

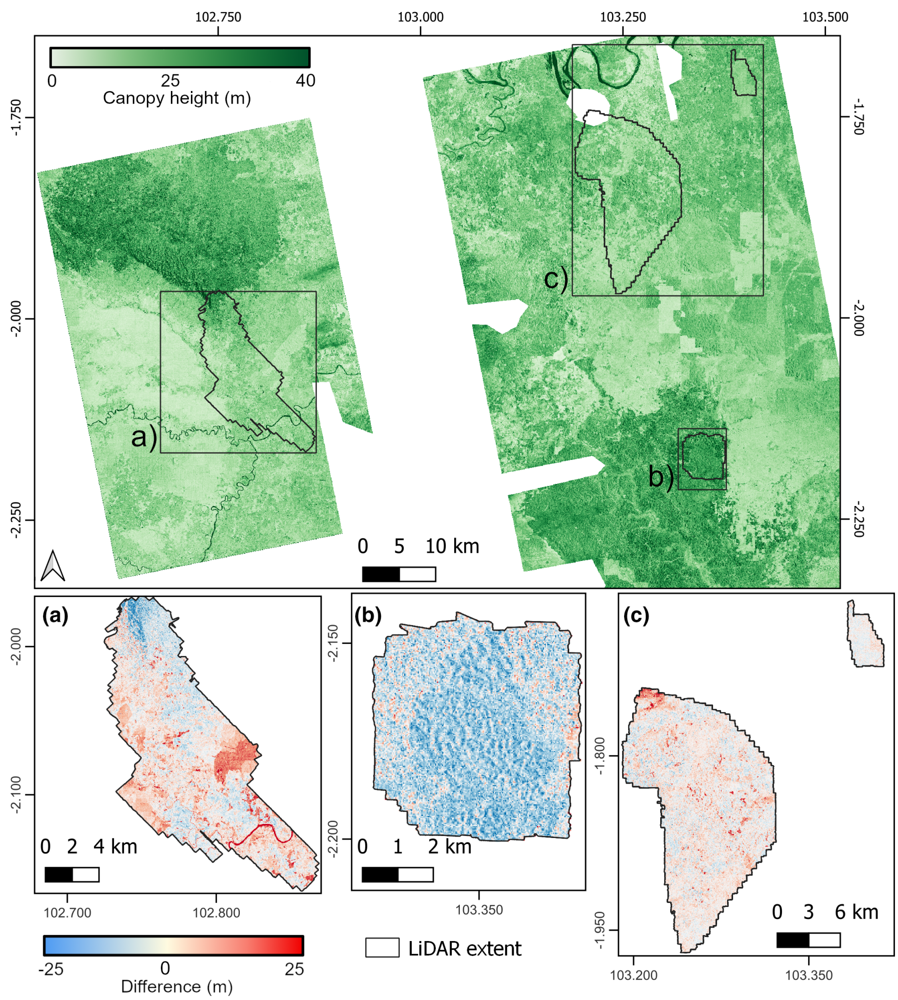

FIGURE 5 Spatial representation of estimated canopy height with the sinc model with empirical parametrization mosaicked for the four TanDEM-X acquisitions (top) and zoom-ins (bottom; a–c) into the extent of the ALS data used as a reference to calculate the difference with the estimated canopy height based on the sinc model with empirical parametrization.

TABLE 4 R^2 and coefficients in multiple-linear regression-models of residuals in the canopy height estimation ΔCHM in relation to ALS canopy height CHM_{ALS}, vegetation cover, effective number of layers (ENL), rumple and standard deviation of heights $SD_{CHM_{ALS}}$ within plots (bold terms were significant with $p<0.001$, Int. stands for intercept)

	R^2	Int.	CHM_{ALS}	Cover	ENL	Rumple	SD_{CHMALS}
$\Delta CHM_{SincEmp_{Scale}}$	0.38	**4.63**	**3.28**	**−0.97**	0.24	−0.18	−0.82
$\Delta CHM_{Sinc_{Scale}}$	0.18	**4.15**	0.31	**−1.47**	0.01	−0.43	1.37
$\Delta CHM_{LinearEmp_{Scale}}$	0.14	**5.59**	**2.86**	0.15	−0.83	−0.23	−0.44
$\Delta CHM_{Linear_{Scale}}$	0.40	**8.92**	**5.87**	0.62	−0.74	0.30	**−2.90**

standard deviations of land-use types were represented for the sake of clarity (Figure 6).

The models as well as the residuals per actual canopy height class suggested that higher canopy heights resulted in higher residuals (Figure 7). The linear model generally underestimated the canopy height irrespective of canopy height and vegetation cover class, in which the smallest canopy heights and vegetation cover were the exception. The sinc model overestimated the canopy height in small canopy height classes up to 20 m, whereas the canopy height was underestimated in actual canopy heights above 20 m. In general, the empirical parametrization improved the estimation for both model variants across all canopy height and vegetation cover classes (Figure 7).

3.4 | Accuracy of canopy height estimation with respect to land-use types

The spatial representation of the residuals between estimated and ALS canopy height indicated that differences were also related to their land use. This was confirmed when the residuals were extracted in the different land-use plots. The canopy height was generally underestimated in the forest plots (Figure 8d), whereas no particular under- or overestimation was observed in the other land uses. The exception was the linear model, which resulted in an underestimation in all land-use types. In general, the highest accuracies were achieved in oil palm plantations followed by rubber, shrubland and forests (Figure 8).

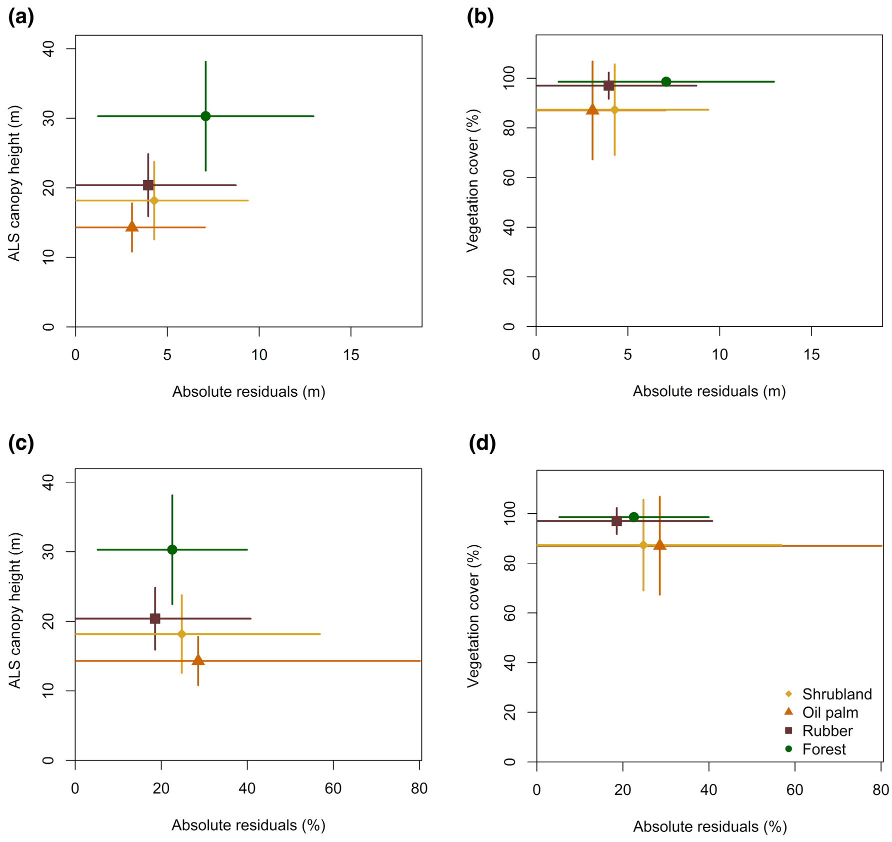

FIGURE 6 Absolute residuals in m [(a) and (b)] and in % [(c) and (d)] of the canopy height estimations in the different land use type plots in relation to the ALS canopy height [(a) and (c)] and vegetation cover [(b) and (d)] (symbols are for the mean and lines for the standard deviation).

The empirical parameterization of the linear model resulted in a substantial improvement, as the differences between the simple linear model and all other models were significant in all land-use types (Figure 8). The linear model had a substantial negative bias in all land uses between −41.1% and −56.6%. The linear parametrization improved the estimations substantially in all land-use types in terms of RMSE and bias (Figure 8). The empirical parameterization of the sinc model improved the accuracy in terms of RMSE and bias in oil palm (33.1% and 16.5% vs. 27.9% and 4.2%) and rubber plantations (26.1% and 15.7% vs. 23.9% and 8%). This resulted in a significant difference of the residuals in these classes. The sinc model without empirical parameterization achieved the highest accuracies in the shrubland plots with an RMSE of 27.8% and a bias of 5.1% and in forest plots with an RMSE of 21.4% and a bias of −9.0% (Figure 8).

One of the assumptions for the simplification of the canopy height estimation model is that the signal has a non-significant extinction. A non-significant extinction was observed in more than 50% of the land-use plots. The highest probability that the extinction was not significant was in oil palm (76%) followed by shrubland (70%) and rubber (67%). These classes had a lower canopy height and lower vegetation cover compared to forests. The majority of the forest plots had a significant extinction, which was indicated by a higher estimated volume coherence $|\gamma_{Vol}|$ than modelled coherence $|\gamma_{Vol_{sinc}}|$ (Table 5).

The forest plots had not just the highest canopy height values but also the highest proportion of land-use plots with a negligible ground contribution from the radar signal (i.e. 23%). A negligible ground contribution is another assumption for the model simplifications. In general, the proportion of land-use plots with negligible ground contribution was low for all land-use types (17%) (Table 5).

4 | DISCUSSION

4.1 | Properties affecting the canopy height estimation with TanDEM-X

Our results confirmed that the conditions on the ground can have a substantial impact on the accuracy of the canopy height estimation with TanDEM-X. The canopy height itself and other structural parameters (mainly vegetation cover) had a significant effect on the accuracies of the canopy height estimation. The effect of vegetation structure is based on the fact that the assumptions for the simplifications of the canopy height estimation models were not valid. This potentially propagated to biased canopy height estimations.

It is assumed in the original models that the coherence is purely based on volume contribution. This means that any residual non-volumetric contribution results in an overestimation (Chen et al., 2016; Guliaev et al., 2021). The non-volumetric compared to the volume contribution is potentially higher in lower than in taller canopy heights. Therefore, a general overestimation of the canopy height was observed until 15–20 m (Figure 7). The parameter *a* in the empirical parametrizations of the canopy height estimation models

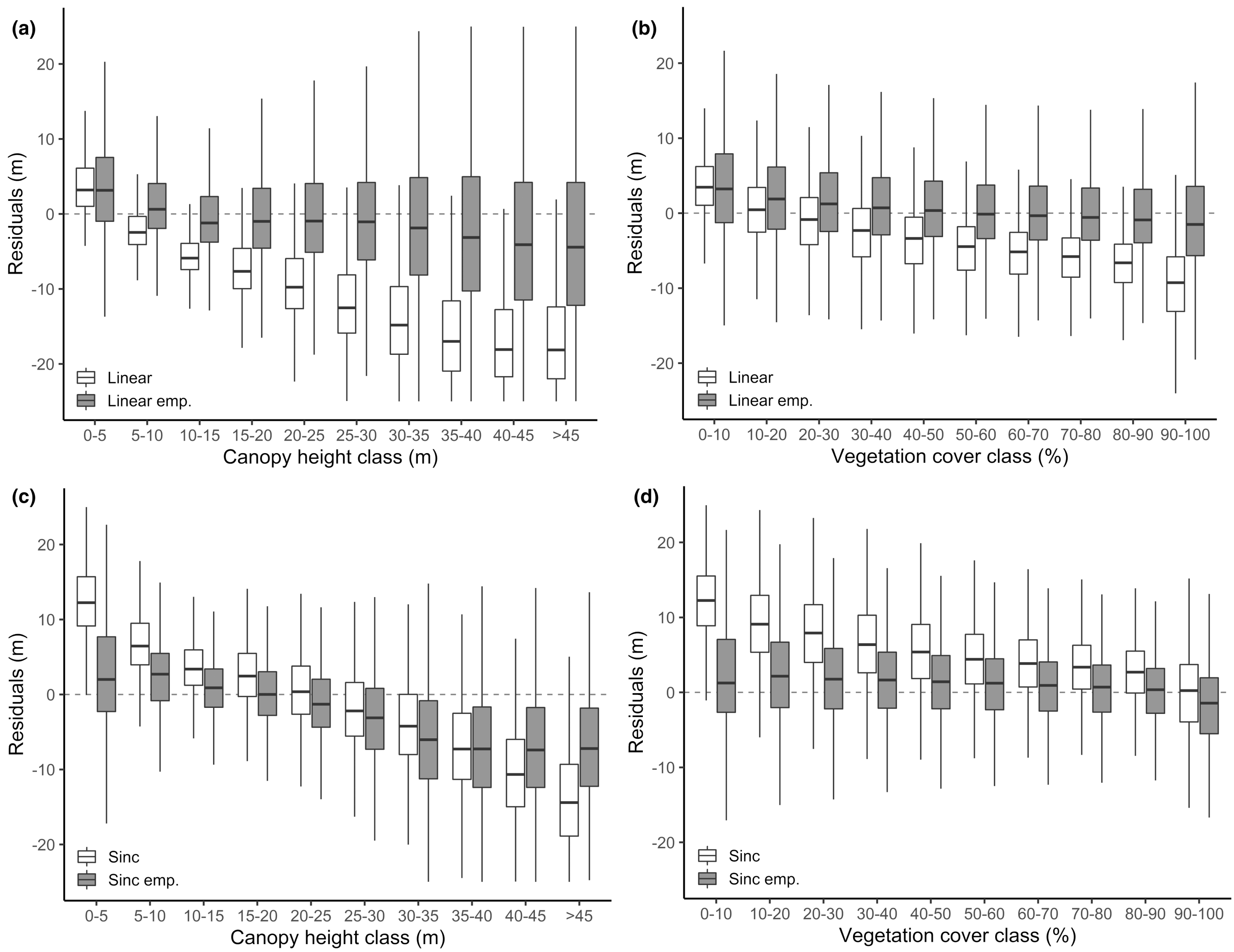

FIGURE 7 Residuals in m per canopy height [(a) and (c)] and vegetation cover class [(b) and (d)] for the linear [(a) and (b)] and sinc [(c) and (d)] model without and with their empirical parametrization in the whole study area (all groups within a class were significantly different).

accounts for that residual non-volumetric contribution in the coherence. Consequently, the overestimation of canopy height decreased in low canopy heights with the empirical parametrization of the models. Another potential cause of the overestimation in small canopy heights is the ground contribution. In the simplified sinc model, no ground contribution is assumed and thus ground contribution (i.e., surface scattering from the ground) results in an overestimation of canopy heights (Chen et al., 2016; Schlund et al., 2019). The overestimation gradually decreases with increasing vegetation cover (Figure 7), where a higher vegetation cover can be assumed to result in a lower probability of ground contribution to the signal.

In contrast to low canopy heights, tall canopy heights were generally associated with an underestimation from TanDEM-X. This is based on the fact that the X-band has limited penetration capabilities into the volume layer of the vegetation (Guliaev et al., 2021). Furthermore, the extinction is assumed to be zero in the simplified models, whereas a significant extinction ($P[|\gamma_{Vol}| < |\gamma_{Vol_{sinc}}|]$) was found in most areas resulting in an underestimation of canopy height (Table 5; Figure 7).

It is important to mitigate the potential biases in the canopy height estimation as those would potentially propagate to ecological applications such as an aboveground biomass estimation based on allometries with canopy height. We generally reduced the over- and underestimation based on these effects by training with GEDI RH100 heights. With regard to canopy height and vegetation cover, the empirical parametrizations generally improved the estimation of canopy height with TanDEM-X reducing effects of residual non-volumetric coherence, ground contribution and extinction of the signal (Figure 7). Previous studies, mostly in higher latitude forests, suggested the possibility to parametrize the simple models with canopy height from ALS (Chen et al., 2021; Gómez et al., 2021; Olesk et al., 2016). Another possibility is the ingestion of ground elevation (Guliaev et al., 2021; Kugler et al., 2014; Qi et al., 2019). It is expected that this is in particular appropriate in taller forests, where the penetration of the TanDEM-X signal is limited. This is why we adopted the model similar to the best case scenario observed by Qi et al. (2019) for GEDI ground elevation and canopy heights at the location of GEDI shots. It can be

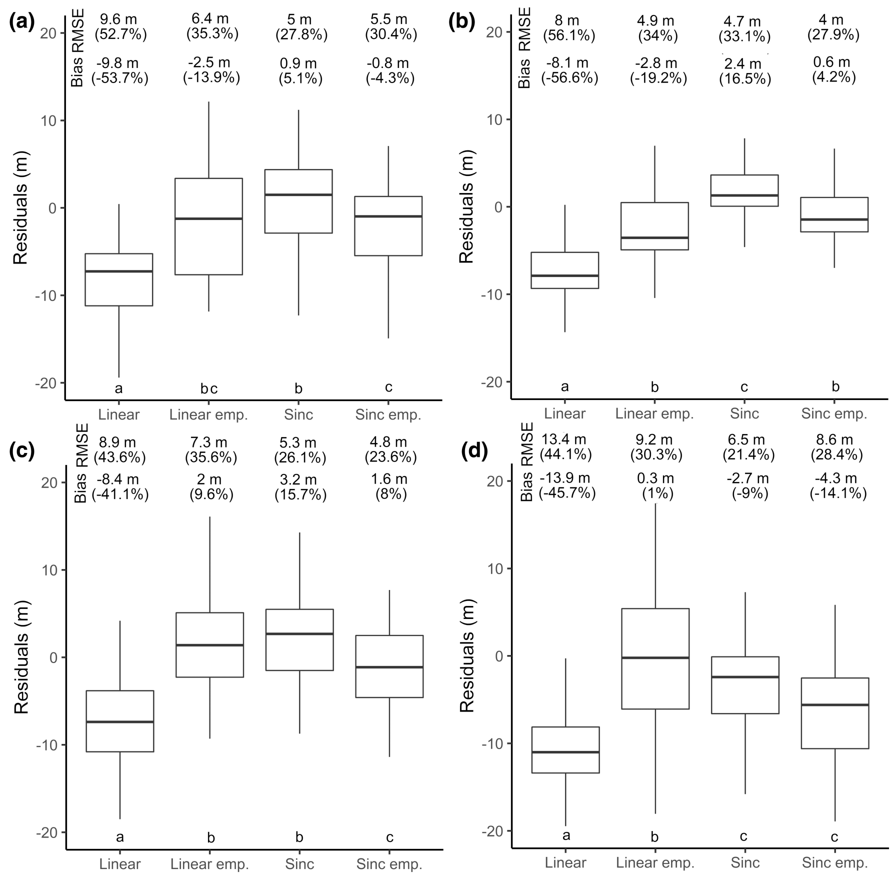

FIGURE 8 Residuals of the canopy height estimations with the different models in the shrubland (a), oil palm (b), rubber (c) and forest (d) land use plots with the RMSE and bias (relative RMSE and bias in brackets).

TABLE 5 Proportion of pixels indicating no ground contribution ($P[h_{\mathrm{InSAR}} > \mathrm{CHM}/2]$) and indicating zero extinction ($P[|\gamma_{\mathrm{Vol}}| < |\gamma_{\mathrm{Vol_{sinc}}}|]$) for all the acquisitions combined in the different land use types with their respective average (and standard devi|ation) canopy height (CHM) and vegetation cover

Land use	$P(h_{\mathrm{InSAR}} >$ CHM/2)	$P(\lvert\gamma_{\mathrm{Vol}}\rvert <$ $\lvert\gamma_{\mathrm{Vol_{sinc}}}\rvert)$	CHM	Veg. cover
Shrubland	0.11	0.70	18.2 (5.7)	87.3 (18.6)
Oil palm	0.17	0.76	14.3 (3.5)	87.1 (20.0)
Rubber	0.17	0.67	20.4 (4.5)	97.0 (5.4)
Forest	0.23	0.28	30.3 (7.9)	98.6 (1.7)
Overall	0.17	0.59	21.1 (8.3)	92.8 (14.5)

assumed that the canopy height estimation with additional ground information is at maximum as good as the ground elevation accuracy itself (Guliaev et al., 2021). Consequently, the accuracies of the simplified models without ground elevation and with ground elevation were not substantially different (Table 2). In general, the previous studies using ALS data and the ground elevation have limited capabilities for a canopy height estimation on large scales, because they relied on sparsely available wall-to-wall ALS data. In contrast, our study explored the potential of spaceborne data, where the models are independent from wall-to-wall canopy height or ground elevation data. This ensures a regional to even global application of these models.

The proportion of pixels indicating no ground contribution ($P[h_{\mathrm{InSAR}} > \mathrm{CHM}/2]$) and zero extinction ($P[|\gamma_{\mathrm{Vol}}| < |\gamma_{\mathrm{Vol_{sinc}}}|]$) was different between the land-use types. The empirical parameters improved the linear model in all land-use types. In contrast, the empirical sinc model outperformed the model without parametrization only for rubber and oil palm (Figure 8). This confirms that a general model is currently not known. It is important to empirically train the models in different land uses and vegetation structures, where the assumptions of the simplifications are not valid (Gómez et al., 2021). Our results suggest that the vegetation and land-use types could be considered for a potential stratification of the empirical parameters of the models. Furthermore, the empirical training of the model parameters could be achieved in smaller local windows instead of the whole scene. Consequently, the local variation of forest structure can be taken into account assuming that a sufficient number of GEDI samples are available.

Bodies of water were an extreme case, where the canopy height estimation models were not valid. Water bodies have generally a very low coherence resulting in very large errors. This confirms that a masking of valid areas can be important for producing reliable results (Schlund et al., 2017). Another source of errors can be identified in the temporal difference between the TanDEM-X and ALS acquisitions, which was visible in the east of Figure 5a. In this particular case, oil palm areas were cleared for re-planting after the end of their production cycle. However, the vast majority did not change substantially between the different acquisition dates.

In addition to the conditions on the ground, the accuracies depend also on acquisition properties (Schlund et al., 2019). It can be assumed that high precipitation and moisture, resulting in high extinction of the signal and a low height of ambiguity can have a negative effect on the canopy height estimation with TanDEM-X (Olesk et al., 2016; Schlund et al., 2019). This was also observed in our study, in particular for the acquisition on 26 April 2019. However, the accuracies of the canopy height estimations with TanDEM-X were generally consistent across the different areas and acquisitions in our study.

4.2 | Canopy height estimation based on different models with TanDEM-X

All TanDEM-X-based canopy height estimations indicated a moderate relationship with the ALS canopy height, where the R^2 ranged from 0.43 to 0.50 resulting in accuracies for the whole landscape in terms of RMSE between 10.3 m (55.8%) to 6.9 m (37.5%) and in terms of bias between −7.3 m (−39.7%) and 2.1 m (11.5%). The relative RMSE was lowest in forests ranging from 21.4% to 44.1%, followed by rubber with 23.6% to 43.6%, oil palm with 27.9% to 56.1% and shrubland with 27.8% to 52.7%. Our canopy height estimation confirms results from higher latitude forests (Chen et al., 2016; Gómez et al., 2021; Olesk et al., 2016; Schlund et al., 2019), in which the simplified models have only been used so far. Similar simplified models without empirical parameters resulted in R^2 values ranging from 0.08 to 0.64 with a relative RMSE ranging from 23.9% to 38.3% in boreal and temperate forests (Schlund et al., 2019). Lower absolute RMSE values ranging from 1.9 to 3.9 m and higher R^2 values ranging from 0.64 to 0.89 were found in the Mediterranean forests, where the empirical parametrization and canopy height estimation was conducted with TanDEM-X and ALS data on forest stand level (Gómez et al., 2021). The density and height of most of those forest stands were substantially lower compared to the tropical forests in our study.

Our study demonstrated the potential of single-polarized TanDEM-X data to estimate vegetation canopy height in a tropical landscape. Other studies in the tropics have exploited dual-polarized or full-polarized TanDEM-X data (Khati et al., 2017, 2018; Kugler et al., 2014). High accuracies with absolute RMSE values of 1.9–2.6 m were achieved with full-polarized TanDEM-X data in Indian forests (Khati et al., 2017, 2018).

The model inversion can be also improved with the ingestion of ground elevation information (Kugler et al., 2014). Based on the limited penetration capability of the X-band, the ground elevation can normally not be derived from TanDEM-X data. Lei et al. (2021) studied the potential to find the ground elevation with TanDEM-X and other data sources in bare areas resulting in a canopy height estimation accuracy of 3.2 m and R^2 of 0.76 on hectare scale. Other studies used ALS data to retrieve the ground elevation (Guliaev et al., 2021; Kugler et al., 2014; Qi et al., 2019; Qi & Dubayah, 2016). For instance, Guliaev et al. (2021) achieved an R^2 at maximum of 0.4 and an absolute RMSE at minimum of 7.4 m by excluding areas with expected underestimation due to the limited penetration capability. Different combination scenarios using the ground elevation and canopy height from GEDI and TanDEM-X were investigated with simulated GEDI data in Qi et al. (2019). This resulted in the best case scenario in a tropical forest study area in an R^2 of 0.44, an RMSE of 4.3 m (13.1%) and a bias of 0.6 m on hectare scale resolution (Qi et al., 2019). We adopted a similar retrieval method to the real GEDI shots in our study area, which resulted in an R^2 of 0.53, an RMSE of 6.1 m (35.8%) and a bias of 0.3 m (2.0%). While the R^2 and bias were comparable or better in our study, the RMSE was higher in our study compared to the reported values in Qi et al. (2019). It is important to note that main differences can be associated to the study area, the resolution (90 m vs. 25 m in our study) and the use of simulated GEDI from ALS in Qi et al. (2019) and actual GEDI data in our study. The accuracy of the ground elevation of the real GEDI data potentially propagated to the canopy height estimation with that ground elevation information (Guliaev et al., 2021). Furthermore, the vegetation cover and canopy height itself have a significant impact on the GEDI canopy height estimation accuracy (Adam et al., 2020). Potential differences between GEDI and ALS canopy height can result in uncertainties in models where GEDI was used for training. Therefore, a selection of GEDI shots with higher sensitivity and accuracy could further improve the results.

Dual- or full-polarized TanDEM-X data and information about the ground elevation is not available with wall-to-wall coverage, high resolution and high accuracy for most parts of the world. Consequently, we studied simple models without any ground elevation information and compared them to a model with ground elevation information. In our study, the empirical parameterization of these simple models with the support of GEDI aimed to account for various extinction and ground-to-volume backscatter ratios. Only a few GEDI footprints within a TanDEM-X acquisition were necessary to train the empirical models. This was in contrast to the approach of Qi et al. (2019), where the kriging of ground elevation information required a generally high density of footprints to estimate the ground accurately on local scale. In contrast to previous studies based on ALS data (Chen et al., 2021; Gómez et al., 2021; Guliaev et al., 2021; Qi et al., 2019), training with the GEDI footprint data potentially enables the large scale application of the TanDEM-X-based canopy height estimation, as demonstrated in our study.

The empirical parameterization of the sinc model was relatively similar compared to the sinc model without empirical parameterization. This was confirmed by model parameters a and b_{sinc} being close to 1. The almost identical models resulted in the fact that the accuracy improved not substantial between the sinc models. This suggested that even if no GEDI footprint would be available (e.g. based on consistent cloud cover), the sinc model would still achieve an accuracy of about 40% in our study.

It is worth noting that Potapov et al. (2021) used the combination of optical Landsat and GEDI data to estimate canopy height on large scales. However, SAR data are considered to have higher potential to estimate canopy height compared to optical data. The combination of the different datasources could be investigated to further improve the canopy height estimation. Our study confirms the potential of TanDEM-X for estimating the canopy height of tropical vegetation.

It can be assumed that the canopy height is related to other forest structural parameters (e.g. aboveground biomass) and biological diversity. Therefore, it is recognized as essential biodiversity variable to be estimated from space (Skidmore et al., 2021). The retrieval of wall-to-wall canopy height on a regional or even global scale is, to date, limited and associated with high uncertainties (Dubayah et al., 2020; Quegan et al., 2019). The canopy height estimation of GEDI and TanDEM-X suggests a potential approach to estimate aboveground biomass on a regional to even global scale with high resolution (Caicoya et al., 2016; Choi et al., 2021; Dubayah et al., 2020). In addition to aboveground biomass, the vegetation canopy height is an important proxy for ecosystem structure and biodiversity (Atkins et al., 2021; Fahey et al., 2019; Lang et al., 2022). It can be assumed that the combination of GEDI and TanDEM-X data could support the assessment of biodiversity with wall-to-wall canopy height information on a regional to global scale (Dubayah et al., 2020). The utilization of two spaceborne systems enables not only the estimation on large scales, but also the consistent monitoring of canopy height and its associated changes over time (Schlund et al., 2021; Solberg et al., 2015). The accuracies of the canopy height estimation with GEDI and TanDEM-X might not be practical for all applications, where dedicated SAR missions could further improve the results in the future (Janoth et al., 2019; Moreira et al., 2015; Quegan et al., 2019; Yu & Saatchi, 2016). At a minimum, the wall-to-wall information based on GEDI and TanDEM-X facilitates the assessment of the spatial distribution of canopy height. This can support forest administrations to identify and monitor vulnerable areas, which are worth to protect. Furthermore, the estimations of canopy height can be classified in qualitative canopy height classes. The canopy height estimation and classification over time can be used to monitor the forest condition and conservation activities. The qualitative canopy height classes can be further used by forest administrations and other stakeholders to support a stratification of ecosystem structure and for efficient forest inventories.

5 | CONCLUSIONS

This study indicated that vegetation canopy height can be estimated wall-to-wall on a regional level with TanDEM-X. The estimation was based on models with different levels of simplification and their empirical parameterization. We demonstrated the potential of TanDEM-X in combination with GEDI data for estimating canopy height in a tropical landscape. The highest overall accuracy was achieved with an empirically trained sinc model. Our results suggested that acquisition properties and conditions on the ground are important for the accurate estimation of canopy height. The training in our study was based on GEDI data, which is an almost globally acquiring spaceborne mission with a sampling concept. The TanDEM-X mission globally acquired data multiple times and thus our study showcases the potential of wall-to-wall canopy height estimation on a regional to even global scale. Our results demonstrate that the combination of both data sources can result in an improved vegetation canopy height information in terms of spatial coverage and accuracy compared to the estimation of canopy height with both data sources alone. Large-scale information on vegetation canopy height could provide essential information to estimate aboveground biomass as well as to monitor forest degradation and restoration. Furthermore, the canopy height is recognized as an essential biodiversity variable (Skidmore et al., 2021). Therefore, the information about canopy height on large scales is also important for applications like forest management and conservation. The results could also be of relevance for future missions with InSAR capabilities in various bands, such as the High Resolution Wide Swath (HRWS), the NISAR, the TanDEM-L and the BIOMASS mission (Janoth et al., 2019; Moreira et al., 2015; Quegan et al., 2019; Yu & Saatchi, 2016), and their combination with GEDI data.

AUTHORS' CONTRIBUTIONS

M.S. and S.E. conceived the ideas and designed methodology; M.S., A.W., N.C. and C.S. collected and processed the data; M.S. analysed the data and led the writing of the manuscript. All authors contributed critically to the drafts and gave final approval for publication.

ACKNOWLEDGEMENTS

This study was funded by the Deutsche Forschungsgemeinschaft (DFG, German Research Foundation)—project number 192626868—SFB 990 and the Ministry of Research, Technology and Higher Education (Ristekdikti) in the framework of the collaborative German—Indonesian research project CRC990, subprojects A03, B09 and Z02. We thank local assistants for support with fieldwork, as well as village leaders, local plot owners, PT REKI, and the Indonesian Research Foundation (LIPI) for research permissions. TanDEM-X data used within this work were provided by DLR under proposal XTI_VEGE7394.

CONFLICT OF INTEREST

The authors have no competing interests to declare.

PEER REVIEW

The peer review history for this article is available at https://publons.com/publon/10.1111/2041-210X.13933.

DATA AVAILABILITY STATEMENT

The LiDAR data is archived in the Göttingen Research Online repository of the CRC990 project: https://doi.org/10.25625/NWX23T (Camarretta, Knohl, et al., 2021) and https://doi.org/10.25625/HWTBW5 (Camarretta et al., 2022). TanDEM-X CoSSC data can generally be requested and accessed at the Science Service System and EOWEB GeoPortal of the German Aerospace Center

(DLR) (DLR, 2021, 2022). GEDI data can be accessed at the Land Processes Distributed Active Archive Center (LP DAAC) of the U.S. Geological Survey (USGS) and the National Aeronautics and Space Administration (NASA) (USGS, 2022).

ORCID

Michael Schlund https://orcid.org/0000-0001-6657-6713

REFERENCES

Adam, M., Urbazaev, M., Dubois, C., & Schmullius, C. (2020). Accuracy assessment of GEDI terrain elevation and canopy height estimates in European temperate forests: Influence of environmental and acquisition parameters. *Remote Sensing*, *12*, 1–28. https://doi.org/10.3390/rs12233948

Asner, G. P., & Mascaro, J. (2014). Mapping tropical forest carbon: Calibrating plot estimates to a simple LiDAR metric. *Remote Sensing of Environment*, *140*, 614–624. https://doi.org/10.1016/j.rse.2013.09.023

Atkins, J. W., Walter, J. A., Stovall, A. E. L., Fahey, R. T., & Gough, C. M. (2021). Power law scaling relationships link canopy structural complexity and height across forest types. *Functional Ecology*, *36*, 713–726. https://doi.org/10.1111/1365-2435.13983

Caicoya, A. T., Kugler, F., Hajnsek, I., & Papathanassiou, K. P. (2016). Large-scale biomass classification in boreal forests with TanDEM-X data. *IEEE Transactions on Geoscience and Remote Sensing*, *54*, 5935–5951. https://doi.org/10.1109/TGRS.2016.2575542

Camarretta, N., Ehbrecht, M., Seidel, D., Wenzel, A., Zuhdi, M., Merk, M. S., Schlund, M., Erasmi, S., & Knohl, A. (2021). Using airborne laser scanning to characterize land-use systems in a tropical landscape based on vegetation structural metrics. *Remote Sensing*, *13*, 1–23. https://doi.org/10.3390/rs13234794

Camarretta, N., Knohl, A., Erasmi, S., & Schlund, M. (2022). *Rasters for ALS metrics at 10 m resolution*. https://doi.org/10.25625/HWTBW5.

Camarretta, N., Knohl, A., Erasmi, S., Schlund, M., Seidel, D., & Ehbrecht, M. (2021). *ALS metrics for Landscape Assessment (LA) plots within LiDAR boundaries*. https://doi.org/10.25625/NWX23T.

Chen, H., Cloude, S. R., & Goodenough, D. G. (2016). Forest canopy height estimation using TanDEM-X coherence data. *IEEE Journal of Selected Topics in Applied Earth Observations and Remote Sensing*, *9*, 3177–3188. https://doi.org/10.1109/JSTARS.2016.2582722

Chen, H., Cloude, S. R., & White, J. C. (2021). Using GEDI waveforms for improved TanDEM-X forest height mapping: A combined SINC + Legendre approach. *Remote Sensing*, *13*, 1–12. https://doi.org/10.3390/rs13152882

Choi, C., Pardini, M., Heym, M., & Papathanassiou, K. (2021). Improving forest height-to-biomass allometry with structure information: A TanDEM-X study. *IEEE Journal of Selected Topics in Applied Earth Observations and Remote Sensing*, *14*, 10415–10427. https://doi.org/10.1109/JSTARS.2021.3116443

Cloude, S., & Papathanassiou, K. (1998). Polarimetric SAR interferometry. *IEEE Transactions on Geoscience and Remote Sensing*, *36*, 1551–1565. https://doi.org/10.1109/36.718859

Cloude, S., & Papathanassiou, K. (2003). Three-stage inversion process for polarimetric SAR interferometry. *IEE Proceedings—Radar, Sonar and Navigation*, *150*, 125–134. https://doi.org/10.1049/ip-rsn:20030449

Clough, Y., Krishna, V. V., Corre, M. D., Darras, K., Denmead, L. H., Meijide, A., Moser, S., Musshoff, O., Steinebach, S., Veldkamp, E., Allen, K., Barnes, A. D., Breidenbach, N., Brose, U., Buchori, D., Daniel, R., Finkeldey, R., Harahap, I., Hertel, D., … Scheu, S. (2016). Land-use choices follow profitability at the expense of ecological functions in Indonesian smallholder landscapes. *Nature Communications*, *7*, 1–12. https://doi.org/10.1038/ncomms13137

Dall, J. (2007). InSAR elevation bias caused by penetration into uniform volumes. *IEEE Transactions on Geoscience and Remote Sensing*, *45*, 2319–2324. https://doi.org/10.1109/TGRS.2007.896613

DLR. (2021). *TanDEM-X science service system*. Retrieved from https://tandemx-science.dlr.de/

DLR. (2022). *EOWEB GeoPortal*. Retrieved from https://eoweb.dlr.de/egp/

Drescher, J., Rembold, K., Allen, K., Beckschäfer, P., Buchori, D., Clough, Y., Faust, H., Fauzi, A. M., Gunawan, D., Hertel, D., Irawan, B., Jaya, I. N. S., Klarner, B., Kleinn, C., Knohl, A., Kotowska, M. M., Krashevska, V., Krishna, V., Leuschner, C., … Scheu, S. (2016). Ecological and socio-economic functions across tropical land use systems after rainforest conversion. *Philosophical Transactions of the Royal Society B: Biological Sciences*, *371*, 20150275. https://doi.org/10.1098/rstb.2015.0275

Dubayah, R., Blair, J. B., Goetz, S., Fatoyinbo, L., Hansen, M., Healey, S., Hofton, M., Hurtt, G., Kellner, J., Luthcke, S., Armston, J., Tang, H., Duncanson, L., Hancock, S., Jantz, P., Marselis, S., Patterson, P. L., Qi, W., & Silva, C. (2020). The Global Ecosystem Dynamics Investigation: High-resolution laser ranging of the Earth's forests and topography. *Science of Remote Sensing*, *1*, 100002. https://doi.org/10.1016/j.srs.2020.100002

Dubayah, R., Hofton, M., Blair, J. B., Armston, J., Tang, H., & Luthcke, S. (2021). *GEDI L2A elevation and height metrics data global footprint level V002* [Data set]. NASA EOSDIS Land Processes DAAC. https://doi.org/10.5067/GEDI/GEDI02_A.002

Ehbrecht, M., Schall, P., Juchheim, J., Ammer, C., & Seidel, D. (2016). Effective number of layers: A new measure for quantifying three-dimensional stand structure based on sampling with terrestrial LiDAR. *Forest Ecology and Management*, *380*, 212–223. https://doi.org/10.1016/j.foreco.2016.09.003

Fahey, R. T., Atkins, J. W., Gough, C. M., Hardiman, B. S., Nave, L. E., Tallant, J. M., Nadehoffer, K. J., Vogel, C., Scheuermann, C. M., Stuart-Haëntjens, E., Haber, L. T., Fotis, A. T., Ricart, R., & Curtis, P. S. (2019). Defining a spectrum of integrative trait-based vegetation canopy structural types. *Ecology Letters*, *22*, 2049–2059. https://doi.org/10.1111/ele.13388

Fatoyinbo, T., Armston, J., Simard, M., Saatchi, S., Denbina, M., Lavalle, M., Hofton, M., Tang, H., Marselis, S., Pinto, N., Hancock, S., Hawkins, B., Duncanson, L., Blair, B., Hansen, C., Lou, Y., Dubayah, R., Hensley, S., Silva, C., … Hibbard, K. (2021). The NASA AfriSAR campaign: Airborne SAR and lidar measurements of tropical forest structure and biomass in support of current and future space missions. *Remote Sensing of Environment*, *264*, 112533. https://doi.org/10.1016/j.rse.2021.112533

Feng, G., Zhang, J., Girardello, M., Pellissier, V., & Svenning, J. C. (2020). Forest canopy height co-determines taxonomic and functional richness, but not functional dispersion of mammals and birds globally. *Global Ecology and Biogeography*, *29*, 1350–1359. https://doi.org/10.1111/geb.13110

Fritz, T. (2012). *TanDEM-X. Ground segment. TanDEM-X experimental product description. Issue: 1.2*. Deutsches Zentrum fuer Luft- und Raumfahrt (DLR).

Gatti, R. C., Paola, A. D., Bombelli, A., Noce, S., & Valentini, R. (2017). Exploring the relationship between canopy height and terrestrial plant diversity. *Plant Ecology*, *218*, 899–908. https://doi.org/10.1007/s11258-017-0738-6

GCOS. (2015). *Status of the global observing system for climate*. WMO. GCOS-195.

Gómez, C., Lopez-Sanchez, J. M., Romero-Puig, N., Zhu, J., Fu, H., He, W., Xie, Y., & Xie, Q. (2021). Canopy height estimation in mediterranean forests of Spain with TanDEM-X data. *IEEE Journal of Selected Topics in Applied Earth Observations and Remote Sensing*, *14*, 2956–2970. https://doi.org/10.1109/JSTARS.2021.3060691

Grass, I., Kubitza, C., Krishna, V. V., Corre, M. D., Mußhoff, O., Pütz, P., Drescher, J., Rembold, K., Ariyanti, E. S., Barnes, A. D., Brinkmann, N., Brose, U., Brümmer, B., Buchori, D., Daniel, R., Darras, K. F. A., Faust, H., Fehrmann, L., Hein, J., … Wollni, M. (2020). Trade-offs between multifunctionality and profit in tropical smallholder landscapes. *Nature Communications*, *11*, 1186. https://doi.org/10.1038/s41467-020-15013-5

Guillaume, T., Kotowska, M. M., Hertel, D., Knohl, A., Krashevska, V., Murtilaksono, K., Scheu, S., & Kuzyakov, Y. (2018). Carbon costs and benefits of Indonesian rainforest conversion to plantations. *Nautre Communications*, *9*, 1–11. https://doi.org/10.1038/s41467-018-04755-y

Guliaev, R., Cazcarra-Bes, V., Pardini, M., & Papathanassiou, K. (2021). Forest height estimation by means of TanDEM-X InSAR and waveform lidar data. *IEEE Journal of Selected Topics in Applied Earth Observations and Remote Sensing*, *14*, 3084–3094. https://doi.org/10.1109/JSTARS.2021.3058837

Janoth, J., Jochum, M., Petrat, L., & Knigge, T. (2019). High resolution wide swath—The next generation X-band mission. In *IEEE International Geoscience and Remote Sensing Symposium (IGARSS)* (pp. 3535–3537). IEEE. https://doi.org/10.1109/IGARSS.2019.8898109

Karila, K., Vastaranta, M., Karjalainen, M., & Kaasalainen, S. (2015). TanDEM-X interferometry in the prediction of forest inventory attributes in managed boreal forests. *Remote Sensing of Environment*, *159*, 259–268. https://doi.org/10.1016/j.rse.2014.12.012

Khati, U., Singh, G., & Ferro-Famil, L. (2017). Analysis of seasonal effects on forest parameter estimation of Indian deciduous forest using TerraSAR-X PolInSAR acquisitions. *Remote Sensing of Environment*, *199*, 265–276. https://doi.org/10.1016/j.rse.2017.07.019

Khati, U., Singh, G., & Kumar, S. (2018). Potential of space-borne PolinSAR for forest canopy height estimation over India—A case study using fully polarimetric L-, C-, and X-band SAR data. *IEEE Journal of Selected Topics in Applied Earth Observations and Remote Sensing*, *11*, 2406–2416. https://doi.org/10.1109/JSTARS.2018.2835388

Krieger, G., Moreira, A., Fiedler, H., Hajnsek, I., Werner, M., Younis, M., & Zink, M. (2007). TanDEM-X: A satellite formation for high-resolution SAR interferometry. *IEEE Transactions on Geoscience and Remote Sensing*, *45*, 3317–3341. https://doi.org/10.1109/TGRS.2007.900693

Kugler, F., Schulze, D., Hajnsek, I., Pretzsch, H., & Papathanassiou, K. (2014). TanDEM-X Pol-InSAR performance for forest height estimation. *IEEE Transactions on Geoscience and Remote Sensing*, *52*, 6404–6422. https://doi.org/10.1109/TGRS.2013.2296533

Lachaise, M., Bachmann, M., Fritz, T., Huber, M., Schweißhelm, B., & Wessel, B. (2019). Generation of the Tandem-X change dem from the new global acquisitions (2017–2019). In *IGARSS 2019–2019 IEEE International Geoscience and Remote Sensing Symposium* (pp. 4480–4483). IEEE. https://doi.org/10.1109/IGARSS.2019.8900192

Lang, N., Kalischek, N., Armston, J., Schindler, K., Dubayah, R., & Wegner, J. D. (2022). Global canopy height regression and uncertainty estimation from GEDI LIDAR waveforms with deep ensembles. *Remote Sensing of Environment*, *268*, 112760. https://doi.org/10.1016/j.rse.2021.112760

Lei, Y., Treuhaft, R., & Gonçalves, F. (2021). Automated estimation of forest height and underlying topography over a Brazilian tropical forest with single-baseline single-polarization TanDEM-X SAR interferometry. *Remote Sensing of Environment*, *252*, 112132. https://doi.org/10.1016/j.rse.2020.112132

Lindgren, N., Persson, H. J., Nystrom, M., Nystrom, K., Grafstrom, A., Muszta, A., Willen, E., Fransson, J. E. S., Stahl, G., & Olsson, H. (2017). Improved prediction of forest variables using data assimilation of interferometric synthetic aperture radar data. *Canadian Journal of Remote Sensing*, *43*, 374–383. https://doi.org/10.1080/07038992.2017.1356220

Meijide, A., Badu, C. S., Moyano, F., Tiralla, N., Gunawan, D., & Knohl, A. (2018). Impact of forest conversion to oil palm and rubber plantations on microclimate and the role of the 2015 ENSO event. *Agricultural and Forest Meteorology*, *252*, 208–219.

Miller, R. G. (1981). *Simultaneous Statistical Inference* (2nd ed.). Springer. https://doi.org/10.1007/978-1-4613-8122-8

Moreira, A., Krieger, G., Hajnsek, I., Papathanassiou, K., Younis, M., Lopez-Dekker, P., Huber, S., Villano, M., Pardini, M., Eineder, M., Zan, F. D., & Parizzi, A. (2015). Tandem-L: A highly innovative bistatic SAR mission for global observation of dynamic processes on the earth's surface. *IEEE Geoscience and Remote Sensing Magazine*, *3*, 8–23. https://doi.org/10.1109/MGRS.2015.2437353

Olesk, A., Praks, J., Antropov, O., Zalite, K., Arumae, T., & Voormansik, K. (2016). Interferometric SAR coherence models for characterization of hemiboreal forests using TanDEM-X data. *Remote Sensing*, *8*, 1–23.

Papathanassiou, K., & Cloude, S. (2001). Single-baseline polarimetric SAR interferometry. *IEEE Transactions on Geoscience and Remote Sensing*, *39*, 2352–2363. https://doi.org/10.1109/36.964971

Parker, G. G., Harmon, M. E., Lefsky, M. A., Chen, J., van Pelt, R., Weiss, S. B., Thomas, S. C., Winner, W. E., Shaw, D. C., & Franklin, J. F. (2004). Three-dimensional structure of an old-growth Pseudotsuga-tsuga canopy and its implications for radiation balance, microclimate, and gas exchange. *Ecosystems*, *7*, 440–453.

Potapov, P., Li, X., Hernandez-Serna, A., Tyukavina, A., Hansen, M. C., Kommareddy, A., Pickens, A., Turubanova, S., Tang, H., Silva, C. E., Armston, J., Dubayah, R., Blair, J. B., & Hofton, M. (2021). Mapping global forest canopy height through integration of GEDI and Landsat data. *Remote Sensing of Environment*, *253*, 112165. https://doi.org/10.1016/j.rse.2020.112165

Praks, J., Antropov, O., & Hallikainen, M. T. (2012). LIDAR-Aided SAR interferometry studies in boreal forest: scattering phase center and extinction coefficient at X- and L-band. *IEEE Transactions on Geoscience and Remote Sensing*, *50*, 3831–3843. https://doi.org/10.1109/TGRS.2012.2185803

Qi, W., & Dubayah, R. O. (2016). Combining Tandem-X InSAR and simulated GEDI lidar observations for forest structure mapping. *Remote Sensing of Environment*, *187*, 253–266. https://doi.org/10.1016/j.rse.2016.10.018

Qi, W., Lee, S. K., Hancock, S., Luthcke, S., Tang, H., Armston, J., & Dubayah, R. (2019). Improved forest height estimation by fusion of simulated GEDI Lidar data and TanDEM-X InSAR data. *Remote Sensing of Environment*, *221*, 621–634. https://doi.org/10.1016/j.rse.2018.11.035

Quegan, S., Le Toan, T., Chave, J., Dall, J., Exbrayat, J. F., Minh, D. H. T., Lomas, M., D'Alessandro, M. M., Paillou, P., Papathanassiou, K., Rocca, F., Saatchi, S., Scipal, K., Shugart, H., Smallman, T. L., Soja, M. J., Tebaldini, S., Ulander, L., Villard, L., & Williams, M. (2019). The European Space Agency BIOMASS mission: Measuring forest above-ground biomass from space. *Remote Sensing of Environment*, *227*, 44–60. https://doi.org/10.1016/j.rse.2019.03.032

Réjou-Méchain, M., Tymen, B., Blanc, L., Fauset, S., Feldpausch, T. R., Monteagudo, A., Phillips, O. L., Richard, H., & Chave, J. (2015). Using repeated small-footprint LiDAR acquisitions to infer spatial and temporal variations of a high-biomass Neotropical forest. *Remote Sensing of Environment*, *169*, 93–101. https://doi.org/10.1016/j.rse.2015.08.001

Schlund, M., & Boehm, H. D. V. (2021). Assessment of linear relationships between TanDEM-X coherence and canopy height as well as aboveground biomass in tropical forests. *International Journal of Remote Sensing*, *42*, 3405–3425. https://doi.org/10.1080/01431161.2020.1871101

Schlund, M., Erasmi, S., & Scipal, K. (2020). Comparison of aboveground biomass estimation from InSAR and LiDAR canopy height models in tropical forests. *IEEE Geoscience and Remote Sensing Letters*, *17*, 367–371. https://doi.org/10.1109/LGRS.2019.2925901

Schlund, M., Kotowska, M. M., Brambach, F., Hein, J., Wessel, B., Camarretta, N., Silalahi, M., Surati Jaya, I. N., Erasmi, S., Leuschner, C., & Kreft, H. (2021). Spaceborne height models reveal above ground biomass changes in tropical landscapes. *Forest Ecology and Management*, *497*, 119497. https://doi.org/10.1016/j.foreco.2021.119497

Schlund, M., Magdon, P., Eaton, B., Aumann, C., & Erasmi, S. (2019). Canopy height estimation with TanDEM-X in temperate and boreal forests. *International Journal of Applied Earth Observation and Geoinformation*, *82*, 101904. https://doi.org/10.1016/j.jag.2019.101904

Schlund, M., Scipal, K., & Davidson, M. W. (2017). Forest classification and impact of BIOMASS resolution on forest area and aboveground biomass estimation. *International Journal of Applied Earth Observation and Geoinformation*, *56*, 65–76. https://doi.org/10.1016/j.jag.2016.12.001

Silva, C. A., Duncanson, L., Hancock, S., Neuenschwander, A., Thomas, N., Hofton, M., Fatoyinbo, L., Simard, M., Marshak, C. Z., Armston, J., Lutchke, S., & Dubayah, R. (2021). Fusing simulated GEDI, ICESat-2 and NISAR data for regional aboveground biomass mapping. *Remote Sensing of Environment*, *253*, 112234. https://doi.org/10.1016/j.rse.2020.112234

Skidmore, A. K., Coops, N. C., Neinavaz, E., Ali, A., Schaepman, M. E., Paganini, M., Kissling, W. D., Vihervaara, P., Darvishzadeh, R., Feilhauer, H., Fernandez, M., Fernández, N., Gorelick, N., Geijzendorffer, I., Heiden, U., Heurich, M., Hobern, D., Holzwarth, S., Muller-Karger, F. E., ... Wingate, V. (2021). Priority list of biodiversity metrics to observe from space. *Nature Ecology & Evolution*, *5*, 896–906. https://doi.org/10.1038/s41559-021-01451-x

Solberg, S., Astrup, R., Breidenbach, J., Nilsen, B., & Weydahl, D. (2013). Monitoring spruce volume and biomass with InSAR data from TanDEM-X. *Remote Sensing of Environment*, *139*, 60–67. https://doi.org/10.1016/j.rse.2013.07.036

Solberg, S., Weydahl, D., & Astrup, R. (2015). Temporal stability of X-band single-pass InSAR heights in a spruce forest: Effects of acquisition properties and season. *IEEE Transactions on Geoscience and Remote Sensing*, *53*, 1607–1614. https://doi.org/10.1109/TGRS.2014.2346473

Treuhaft, R., Goncalves, F., dos Santos, J., Keller, M., Palace, M., Madsen, S., Sullivan, F., & Graca, P. (2015). Tropical-forest biomass estimation at X-band from the spaceborne TanDEM-X interferometer. *IEEE Geoscience and Remote Sensing Letters*, *12*, 239–243. https://doi.org/10.1109/LGRS.2014.2334140

USGS. (2022). *GEDI02_A v002. GEDI L2A elevation and height metrics data global footprint level*. Retrieved from https://lpdaac.usgs.gov/products/gedi02_av002/

Yu, Y., & Saatchi, S. (2016). Sensitivity of L-band SAR backscatter to aboveground biomass of global forests. *Remote Sensing*, *8*, 1–18.

How to cite this article: Schlund, M., Wenzel, A., Camarretta, N., Stiegler, C., & Erasmi, S. (2023). Vegetation canopy height estimation in dynamic tropical landscapes with TanDEM-X supported by GEDI data. *Methods in Ecology and Evolution*, *14*, 1639–1656. https://doi.org/10.1111/2041-210X.13933